




## Article

# Modified Harmony Search Algorithm-Based Optimization for Eco-Friendly Reinforced Concrete Frames

Gebrail Bekdaş<sup>1,\*</sup>, Sinan Melih Nigdeli<sup>1</sup>, Sanghun Kim<sup>2</sup> and Zong Woo Geem<sup>3,\*</sup>

<sup>1</sup> Department of Civil Engineering, İstanbul University-Cerrahpaşa, İstanbul 34320, Turkey; melihnig@iuc.edu.tr

<sup>2</sup> Department of Civil and Environmental Engineering, Temple University, Philadelphia, PA 19122, USA; sanghun.kim@temple.edu

<sup>3</sup> College of IT Convergence, Gachon University, Seongnam 13120, Korea

\* Correspondence: bekdas@iuc.edu.tr (G.B.); geem@gachon.ac.kr (Z.W.G.)

**Abstract:** Cost and CO<sub>2</sub> are two factors in the optimum design of structures. This study proposes a modified harmony search methodology for optimization of reinforced concrete beams with minimum CO<sub>2</sub> emissions. The optimum design was developed in detail by considering all possible combinations of variable loads, including dynamic force resulting from earthquake motion. Moreover, time-history analyses were performed, and requirements of the ACI-318 building code were considered in the reinforced concrete design. The results show that the optimum design based on CO<sub>2</sub> emission minimization is greatly different from the optimum cost design results. According to these results, using recycled members provides a sustainable design.

**Keywords:** optimization; harmony search; reinforced concrete frames; earthquake; CO<sub>2</sub> emission minimization; cost minimization



**Citation:** Bekdaş, G.; Nigdeli, S.M.; Kim, S.; Geem, Z.W. Modified Harmony Search Algorithm-Based Optimization for Eco-Friendly Reinforced Concrete Frames. *Sustainability* **2022**, *14*, 3361. <https://doi.org/10.3390/su14063361>

Academic Editors: Seungjun Roh, Tae-Hyoung Kim and Jorge de Brito

Received: 21 February 2022

Accepted: 10 March 2022

Published: 13 March 2022

**Publisher's Note:** MDPI stays neutral with regard to jurisdictional claims in published maps and institutional affiliations.



**Copyright:** © 2022 by the authors. Licensee MDPI, Basel, Switzerland. This article is an open access article distributed under the terms and conditions of the Creative Commons Attribution (CC BY) license (<https://creativecommons.org/licenses/by/4.0/>).

## 1. Introduction

Carbon footprint is a measure of the damage caused by human activities to the environment in terms of the amount of greenhouse gas produced, measured in units of carbon dioxide, and consists of two main parts: a direct (primary) footprint and an indirect (secondary) footprint. The primary footprint is a measure of direct CO<sub>2</sub> emissions from the combustion of fossil fuels, including domestic energy consumption and transportation (for example, cars and airplanes). The secondary footprint is indirect CO<sub>2</sub> emissions from the entire life cycle of the products we use, related to their manufacture and eventual degradation.

In an engineering design, a challenging task is to provide additional factors that are not related to compulsory safety requirements. These additional factors may be a minimum cost design or an eco-friendly design. In this manner, safety is a must, and an advantageous design needs an optimum design according to a factor that makes engineering design important.

In the design of reinforced concrete (RC) structures, due to the strength and serviceability requirements in design codes and composite designs of concrete and steel reinforcement, the optimum design problems that minimize cost or CO<sub>2</sub> emissions can only be solved via iterative methods. The best and most time-saving methodology for an iterative finding of different design-variable combinations is provided via metaheuristic methods. Especially for frame members that include both tension-controlled beam members and compressive-controlled column members, the importance of the need for an advanced method becomes evident.

In the optimum design of steel structures, weight optimization can provide a reduction in cost and CO<sub>2</sub> since it is constructed from a single material. The reduction in the material used in the construction will both reduce CO<sub>2</sub> emissions and cost in the same way. This cannot be for RC structures, and cost optimization is needed to find a balance between the

amounts of concrete and steel used [1]. Moreover, this is the reason for the different design concepts of minimizing the amount of CO<sub>2</sub> emissions since the cost and CO<sub>2</sub> emission ratios of concrete and steel are different.

For the cost optimization, Adeli and Sarma [2] reviewed the soft computing applications of optimum RC design, including Genetic Algorithm (GA), fuzzy logic, and parallel computing. GA is the most-used algorithm, and Coello et al. [3] optimized RC beams via GA to achieve a realistic and practical design. By applying a declarative approach that is used to check the exact bending capacities, GA is employed in the optimum design of biaxial columns by Rafiq and Soutcombe [4]. Koumousis and Arsenis [5] aimed to provide sets of rebars of specific diameters instead of a rebar area in their study employing GA for RC members. Rajeev and Krishnamoorthy [6] employed GA for RC frames with discrete variables. Rath et al. [7] employed a natural velocity field method in the shape optimization of RC members under a flexural moment using GA in optimizing rebar variables. Camp et al. [8] optimized RC frames via GA and demonstrated the efficiency of the method for simply supported beams, uniaxial columns, and multi-storey frames. Continuous beams that were optimized via a hybrid algorithm of GA and simulated annealing (SA) were presented by Leps and Sejnoha [9]. Lee and Ahn [10] proposed a GA-based approach for RC plane frames using lateral equivalent static earthquake loads. Govindaraj and Ramasamy [11] optimized RC continuous beams by using GA for cross-section variables and reinforcement templates for rebar variables. Sahab et al. [12] employed GA following the Hook and Jeeves method in the optimization of RC flat slab buildings. Govindraj and Ramasamy [13] developed a method based on GA for RC frames by using a sub-level optimization problem detailing of rebar of beams. For CO<sub>2</sub> minimization, Park et al. [14] optimized RC columns with GA by converting CO<sub>2</sub> emission values into costs using the concept of the certified emissions reductions (CERs). Lee et al. [15] employed GA in the reduction in the cost and CO<sub>2</sub> emissions of RC frames. Mergos [16] employed GA to optimize RC frames via seismic analysis and CO<sub>2</sub> minimization.

Harmony search (HS) is another algorithm that has been widely used in the optimization of RC structures. Akin and Saka [17] proposed a detailed optimization methodology for RC frames by employing HS and considered the provisions in ACI 318-05 [18]. Nigdeli et al. employed HS in the optimization of biaxially loaded RC columns [19]. Bekdaş optimized post-tensioned axially symmetric cylindrical RC walls via HS and considered both post-tension and RC design variables [20]. Garcia Segura et al. proposed a hybrid HS using threshold optimization to optimize the geometry and materials of post-tensioned concrete box-girder pedestrian bridges [21]. Bekdaş and Nigdeli investigated the cost optimization of RC frames subjected to earthquakes by proposing a modified HS [22]. Medeiros and Kripta conducted a discrete optimization for the cost minimization of RC columns via a modified HS [23]. Shaqfa and Orban used a parameter-setting free HS to optimize RC beams for cost and weight objectives [24]. Kayabekir et al. proposed a multi-objective optimization, including cost and CO<sub>2</sub> objectives for RC-retaining walls, and employed HS [25]. Yucel et al. hybridized adaptive HS with the Jaya algorithm in the optimum design of RC-retaining walls [26]. RC cantilever soldier pile-retaining walls have been optimized via HS for cost optimization [27] and multi-objective optimization, including CO<sub>2</sub> emission minimization [28]. Recently, Kayabekir et al. proposed adaptive HS for the cost optimization of RC columns [29].

The algorithms used in the optimum design of RC members are large in number, and only recent applications were mentioned. Nigdeli et al. optimized RC footings via various metaheuristic algorithms, including HS, the flower pollination algorithm (FPA), and teaching–learning-based optimization (TLBO) [30]. Particle swarm optimization (PSO) with multi-criterion decision making was proposed by Esfandari et al. [31] to optimize RC frames subjected to time-history loadings, and the two objectives were taken as cost and weight. RC beams were optimized by Afshari et al. [32] using a multi-objective version of five algorithms, and the objectives were cost and deflection. Mergos and Mantoglou employed FPA for the cost optimization of RC cantilever-type retaining walls [33]. Uray

and Carbas evaluated the optimum design of RC-retaining walls via HS by using different soil characteristics and earthquake loads [34]. Sanchez-Olivares and Tomas employed a modified firefly algorithm and optimized RC members, which were subjected to compression and biaxial bending based on two design codes, including Eurocode 2 and ACI318 [35]. For CO<sub>2</sub> emission minimization, RC footings were optimized via a hybrid big bang–big crunch algorithm (BB–BC) [36]. RC frames were optimized via simulated annealing for CO<sub>2</sub> optimization [37]. BB–BC was also applied to RC frames [38].

In the present study, RC frame structures are optimized according to CO<sub>2</sub> emission minimization by using a modified HS algorithm. This algorithm has been tested on various structural engineering applications and is proven to be an effective algorithm via modifications [17–29]. By dividing the randomization process into stages, the convergence is provided by quickly eliminating the violated results of the design constraints. Moreover, the problem of additional random steps is considered due to complex analysis of the system considering a time-history analysis via seismic loads and combinations of variable action loads.

## 2. Methods

The optimization of RC frames contains the optimum design of multiple structural members. Additionally, these members are of two types: beams and columns. Beams are subjected to bending and designed according to tension-controlled member rules. Columns are subjected to compression and bending and designed according to compressive-controlled member rules.

Generally, in engineering optimization via metaheuristic algorithms, all design variables are randomized, and then the calculations are performed for design constraints and objectives. In the proposed method, the randomization of design variables is conducted in different stages. This methodology employs HS, with additional randomization stages to shorten the optimization process. Due to the existence of various members and types, the analysis for all members is only a time loss if only one constraint is not provided for a member. Additionally, in the case of violation of the final checked constraints, randomization stages that are iteratively conducted for providing the constraints are included. Until violated members are assigned with non-violated design variables, randomization of design variables of the corresponding members is repeated.

The optimization code employing HS is a music-inspired metaheuristic algorithm developed by Geem et al. [39]. The process code was written in Matlab by Simulink [40]. It includes not only the dynamic analysis, but also considers the seismic records downloaded from the PEER database [41]. The optimization includes 4 steps.

In the first step, the design constants are defined. These constants include structural data such as number of bays, stories, and joints with boundary conditions, coordinates of element endpoints, material properties, design variable ranges, and loading conditions. The design variables are cross-section dimensions such as breadth ( $b_w$ ) and height ( $h$ ), and reinforcement amounts such as number and size. The material properties, including the structural protection measures, are clear cover ( $c_c$ ), maximum aggregate diameter ( $D_{max}$ ), elasticity modulus of steel ( $E_s$ ), specific gravity of steel ( $\gamma_s$ ), specific gravity of concrete ( $\gamma_c$ ), compressive strength of concrete ( $f_c$ ), yield strength of steel ( $f_y$ ), unit cost of concrete per m<sup>3</sup> ( $C_c$ ), unit CO<sub>2</sub> emission of concrete per m<sup>3</sup> ( $C_{c,co2}$ ), unit cost of steel per ton ( $C_s$ ), and unit CO<sub>2</sub> emission of steel per ton ( $C_{s,co2}$ ).

In step 2, an initial solution matrix is generated, and the candidate design variables are checked for objective function and design constraints. In this study, the design constraints are calculated according to ACI-318-14 [15]. This step contains 7 sub-steps.

In step 2.1, the randomization process starts with the assignment of cross-sectional dimensions of the beams. The following constraints of Equations (1) and (2) are checked:

$$g_1 = d - \frac{l}{4} < 0 \quad (1)$$

$$g_1 = b_w - 0.3h \geq 0 \quad (2)$$

The depth of the beam is shown as  $d$ , and the clear length of the beam is given as  $l$ . The design variables are randomized for  $b_w$  and  $h$  until these two constraints are provided. The dimensions are discrete variables that are suitable for practical design. Since reinforcement bars are not known, the depth of the beam is taken as 50 mm less than the height.

In step 2.2, the cross-section dimensions of columns are randomized, and Equation (3) is checked. In this equation,  $b$  is the breadth of the supporting column. The randomization of column dimensions is performed until this constraint is provided:

$$g_3 = b_w - b - \frac{3}{2}d \leq 0 \quad (3)$$

In step 2.3, a structural analysis is performed for the defined cross-section dimensions of beams and columns. The optimization involves both static and dynamic analyses. In the analyses, the system matrices are calculated by using the stiffness method. As shown in Equations (4) and (5), mass ( $M_e$ ) and stiffness matrices ( $K_e$ ) of a member are calculated by considering the rotation and two displacements in each joint, without assuming that the system is a shear building for the dynamic analysis:

$$M_e = \frac{\gamma_c A l + (D + nL)(l - a)}{420g} \begin{bmatrix} 140 & 0 & 0 & 70 & 0 & 0 \\ 0 & 156 & 22l & 0 & 54 & -13l \\ 0 & 22l & 4l^2 & 0 & 13l & -3l^2 \\ 70 & 0 & 0 & 140 & 0 & 0 \\ 0 & 54 & 13l & 0 & 156 & -22l \\ 0 & -13l & -3l^2 & 0 & -22l & 4l^2 \end{bmatrix} \quad (4)$$

$$K_e = \begin{bmatrix} \frac{EA}{l} & 0 & 0 & -\frac{EA}{l} & 0 & 0 \\ 0 & \frac{12EI}{l^3} & \frac{6EI}{l^2} & 0 & -\frac{12EI}{l^3} & \frac{6EI}{l^2} \\ 0 & \frac{6EI}{l^2} & \frac{4EI}{l} & 0 & -\frac{6EI}{l^2} & \frac{2EI}{l} \\ -\frac{EA}{l} & 0 & 0 & \frac{EA}{l} & 0 & 0 \\ 0 & -\frac{12EI}{l^3} & -\frac{6EI}{l^2} & 0 & \frac{12EI}{l^3} & -\frac{6EI}{l^2} \\ 0 & \frac{6EI}{l^2} & \frac{2EI}{l} & 0 & -\frac{6EI}{l^2} & \frac{4EI}{l} \end{bmatrix} \quad (5)$$

where  $A$ ,  $I$ ,  $l$ ,  $E$ ,  $n$ , and  $g$  represent the cross-sectional area of the element, moment of inertia of the element, length of the element, modulus of elasticity, live load participation factor, and gravity, respectively.

In the static analysis, including live loads ( $L$ ) that are of variable action, the combinational cases of spans with loadings are considered to calculate the worst internal forces. The self-mass of the beams and columns are added to the dead load ( $D$ ), which is a permanent action.

The dynamic analyses were conducted in Matlab using Simulink [40], and Equation (6) is solved for a ground acceleration defined as  $\ddot{x}_g$ :

$$M\ddot{x}(t) + C\dot{x}(t) + Kx(t) = -M\{1\}\ddot{x}_g(t) \quad (6)$$

where  $x(t)$  is the displacement as shown in the vector, and a dot on it represents derivative with respect to time;  $\{1\}$  is a unit vector of ones. The damping matrix is calculated via the Rayleigh method by considering 5% damping in the first two vibration modes. In the study, three different seismic records are used for a time-history analysis, and internal forces due to earthquake acceleration ( $u$ ) are calculated. Then, these forces are divided into the elastic response parameter ( $R$ ), and the worst condition is searched by using the combination from Equations (7)–(9). The most critical response is used in the design of RC members:

$$U = 1.4D + 1.7L \quad (7)$$

$$U = 0.75(1.4D + 1.7L) \pm E \quad (8)$$

$$U = 0.9D \pm E \quad (9)$$

In step 2.4, the maximum capacity of axial force ( $N_{\max}$ ) and shear force ( $V_{\max}$ ) are controlled for columns to ensure brittle fracture conditions:

$$g_4 = V_{\max} - \min \left\{ \begin{array}{l} 5.5A \\ 0.2f'_cA \end{array} \right\} \leq 0 \quad (10)$$

$$g_5 = N_{\max} - 0.5f'_cA \leq 0 \quad (11)$$

In addition, the following constraint is considered in the optimization for the beams as shown in Equation (12):

$$g_6 = N_{\max} - 0.1f'_cA \leq 0 \quad (12)$$

If the constraints checked in this sub-step are not provided, the candidate dimension values are randomized by considering the other constraints in steps 2.1 and 2.2.

In step 2.5, the longitudinal reinforcements for tensile fiber of beams are randomized. The brittle fracture constraint given as Equation (13) is calculated, and if it is not provided, the randomization of reinforcements for compressive sections of beams is also conducted. The reinforcement ratio is symbolized by  $\rho$ :

$$g_7 = \rho - (0.75)(0.85)\beta_1 \frac{f'_c}{f_y} \left( \frac{600}{600 + f_y} \right) \leq 0 \quad (13)$$

Furthermore, the reinforcement ratio must be suitable for the maximum reinforcement ratio for beams, which is 0.025, as shown in Equation (14):

$$g_8 = \rho - 0.025 \leq 0 \quad (14)$$

In addition, the positioning of reinforcements is controlled. The clear distance between the bars ( $a_\phi$ ) must be provided, as shown in Equation (15):

$$g_9 = a_\phi - \max \left\{ \begin{array}{l} \phi_{\text{average}} \\ 25 \text{ mm} \\ \frac{4}{3}D_{\max} \end{array} \right\} > 0 \quad (15)$$

where  $D_{\max}$  is the maximum size of aggregates used in concrete and  $\phi_{\text{average}}$  is the average value of assigned reinforcement sizes. The optimization code allows for two-line placement of reinforcements.

To reduce the possibility of using reinforcement bars that are more than what is required to provide internal forces for the randomly assigned values, the constraint in Equation (16) is checked.  $A_{s\text{-random}}$  is the reinforcement bars and  $A_{s\text{-needed}}$  is the value calculated for the internal forces:

$$g_{10} = A_{s\text{-random}} - (1 + r)A_{s\text{-needed}} < 0 \quad (16)$$

where  $r$  is a user-defined value. If Equation (16) cannot be provided and  $r$  is not taken as a physical value, the process may become trapped in this step. For that reason,  $r$  value is increased by 0.01 after every 500 iterations of this sub-step. In addition, after 20,000 iterations in this sub-step, the objective function is penalized.

Furthermore, the minimum reinforcement area ( $A_{s,\min}$ ) is provided in this sub-step. These are given as Equations (17) and (18):

$$g_{11} = A_{s,\text{minimum}} - \frac{\sqrt{f'_c}}{4f_y} b_w d \geq 0 \quad (17)$$

$$g_{12} = A_{s,\min} - \frac{1.4}{f_y} b_w d \geq 0 \quad (18)$$

Equations (17) and (18) are considered for both tensile and compressive sections of the beam. For the joint points, the reinforcement in compressive sections must be also half of the reinforcements in tensile sections.

After the design and randomization of longitudinal reinforcements of the beam, shear reinforcements (stirrups) are assigned and the constraints in Equations (19)–(21) are checked:

$$g_{13} = V - \frac{\sqrt{f'_c}}{6} b_w d - \frac{A_v f_y d}{s} \leq 0 \quad (19)$$

$$g_{14} = \frac{A_v f_y d}{s} - 0.66 \sqrt{f'_c} b_w d \leq 0 \quad (20)$$

$$g_{15} = A_v - \frac{1}{3} \frac{b_w s}{f_y} \geq 0 \quad (21)$$

where  $V$ ,  $A_v$ , and  $s$  represent shear force, shear reinforcement area, and spacing of stirrups, respectively. In addition, the  $s$  value must be less than the value of Equation (22) according to the  $V_s$  value, which is the shear force capacity provided by stirrups. The spacing of reinforcements is a discrete variable that is in multiples of 10 mm:

$$g_{16} = \begin{cases} s - \frac{d}{2} \leq 0 & \text{if } V_s \leq 0.33 \sqrt{f'_c} b_w d \\ s - \frac{d}{4} \leq 0 & \text{if } V_s \geq 0.33 \sqrt{f'_c} b_w d \end{cases} \quad (22)$$

In step 2.6, the design of columns is controlled by considering the slenderness effect according to the moment magnification concept. To represent the state just before the ultimate load, the values of moment of inertia are reduced by 65% and 30% for beams and columns, respectively. If the design flexural moment is less than the minimum value ( $M_{\min}$ ) in Equation (23), then the minimum value is used:

$$M_{\min} = P_u(15 + 0.03h) \text{ if } h \text{ in mm} \quad (23)$$

Similarly, the longitudinal reinforcements of the columns are randomly assigned for symmetric reinforcement in the upper and lower fiber of the cross-section. Then, the positioning of reinforcement bars is provided according to Equation (24):

$$g_{17} = a_\phi - \left\{ \begin{array}{c} 1.5\phi_{\text{average}} \\ 40 \text{ mm} \\ \frac{4}{3} D_{\max} \end{array} \right\} \geq 0 \quad (24)$$

If the clear distance between the upper and lower fiber reinforcements is more than 150 mm, web reinforcements are also placed. For columns, the minimum and maximum reinforcement ratios ( $\rho$ ) in Equations (25) and (26) are considered:

$$g_{18} = \rho - 0.06 \leq 0 \quad (25)$$

$$g_{19} = \rho - 0.01 \geq 0 \quad (26)$$

The randomization of column reinforcements is repeated until the constraints in Equations (25) and (26) are provided.

The required capacity of axial force and flexural moment for the candidate design is checked according to a procedure. In this procedure, the distance from the extreme compression fiber to the neutral axis ( $c$ ) is iteratively searched, and the  $c$  value for the lowest flexural moment ensuring the required axial force is stored. This capacity ( $M_{\text{capacity}}$ ) is checked for Equation (27) and the randomization is repeated until it is provided. For the user-defined  $r$  value, the same procedure in the beam design is applied.  $M_{\text{required}}$  is the required design moment value:

$$g_{20} = M_{\text{capacity}} - (1 + r)M_{\text{required}} < 0 \quad (27)$$

As the final sub-step 2.7, the objective function is calculated. For CO<sub>2</sub> emission of an element, Equation (28) is used:

$$C_e = (A_g - A_{st})l_e C_{c,co2} + (A_{st} + \frac{A_v}{s} u_{st})l_e \gamma_s C_{s,co2} \quad (28)$$

where  $C_e$  is the CO<sub>2</sub> emission value of an element.  $A_g$ ,  $A_{st}$ ,  $A_v$ ,  $u_{st}$ , and  $l_e$  are the area of cross-section, area of longitudinal reinforcement, area of shear reinforcement, and length of the element, respectively. The objective function (OF) is calculated by adding all values of CO<sub>2</sub> emission for all elements as shown in Equation (29). For penalized values, OF is assigned as  $10^6$ , which is a very large value:

$$OF = \sum_{i=1}^n (C_e)_i \quad n : \text{number of elements} \quad (29)$$

After all beam and column design variables are assigned and the objective function is calculated for these values, the initial harmony memory (HM) matrix is constructed. This HM matrix contains harmony vectors as the number of harmony memory size (HMS).

In step 3, the essential optimization process starts. New sets of design variables are generated via sub-steps controlling the constraints via iterative randomization to ensure these constraints. As with the modification of HS, harmony memory is considered by changing the boundary limits of design variables. Harmony memory is chosen according to the harmony memory consideration rate (HMCR), and it is taken as 0.5. In the local search, the minimum or maximum range of design variables is updated with the best existing solution ( $X_{best}$ ), with equal probability. Thus, both less and more of the best solution is searched in discrete optimization. The generation of a variable ( $X$ ) with respect to minimum ( $X_{min}$ ) and maximum ( $X_{max}$ ) ranges is formulated as Equation (30). In Equation (30),  $\text{rand}(0, 1)$  is a random number between 0 and 1. It is regenerated in all calculations:

$$X = \begin{cases} X_{min} + \text{rand}(0, 1)[X_{max} - X_{min}] & \text{if } \text{rand}(0, 1) > 0 \\ X_{min} + \text{rand}(0, 1)[X_{best} - X_{min}] & \text{if } \text{rand}(0, 1) < 0 \\ X_{best} + \text{rand}(0, 1)[X_{max} - X_{best}] & \text{if } \text{rand}(0, 1) \geq 0 \end{cases} \quad \text{if } \text{rand}(0, 1) \leq \text{HMCR} \quad (30)$$

As the last step, the newly generated solutions are updated if the OF value for these solutions is smaller than the existing ones. Steps 3 and 4 are applied for the maximum number of iterations. The methodology of the optimization process is summarized in the flowchart in Figure 1.



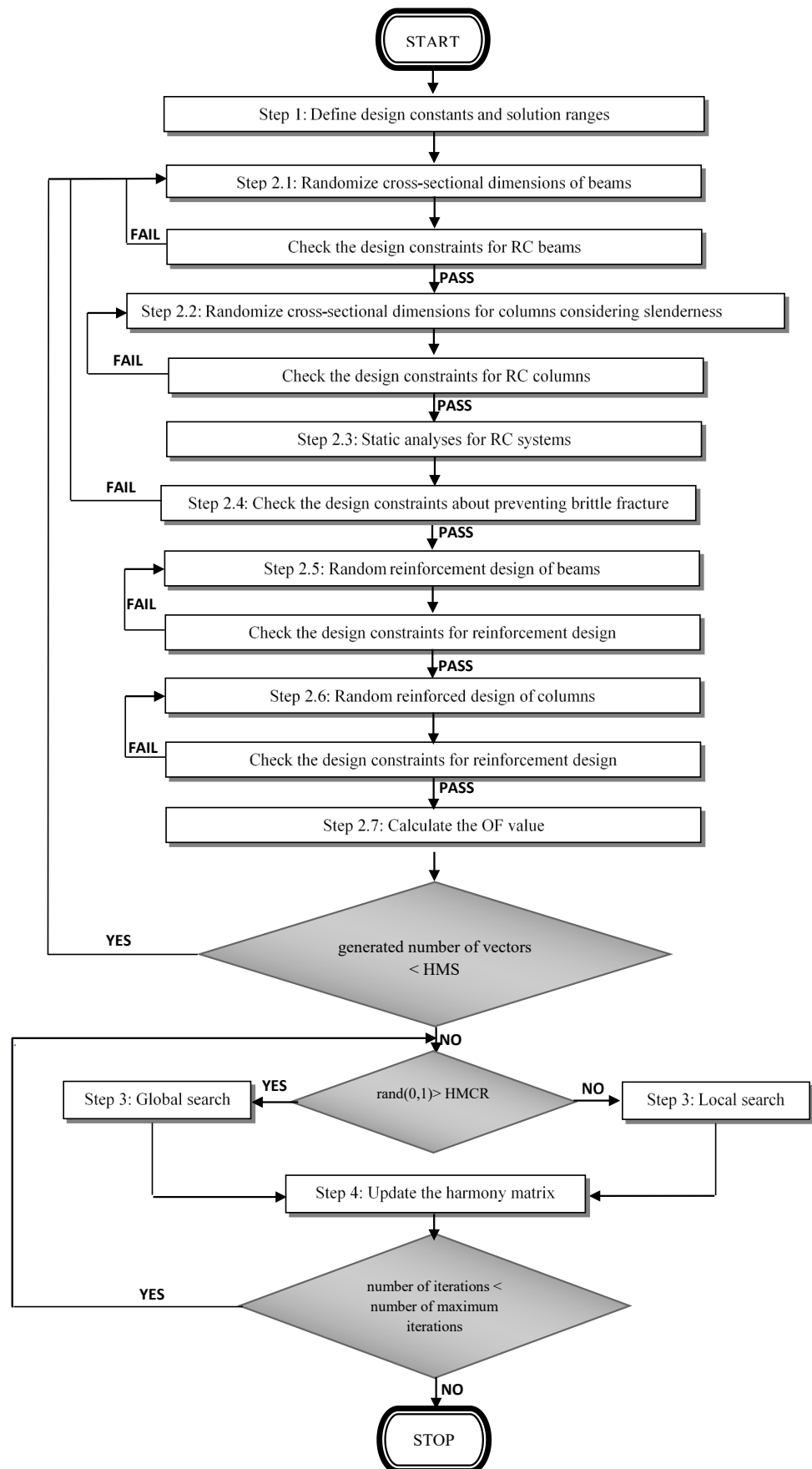


Figure 1. Flowchart of the optimization methodology.



### 3. Results

In the numerical example, a three-storey three-span frame structure, as shown in Figure 2, was optimized. The column bases were fixed. The height of each storey is 3 m from the bottom of part of the slab to the bottom of the upper slab. By considering the load transformation case from slabs to beams, the static loads,  $D$  and  $L$ , were defined as trapezoidal distributed loads. The frame system consists of 21 members (12 columns and 9 beams) that are optimized without grouping. For the dynamic loads, three earthquake records, as shown in Table 1, were considered in the optimization. The optimization is performed for the constant values and design ranges shown in Table 2. The optimization was conducted for cost to compare the results. To promote sustainable development, the value of  $\text{CO}_2$  emission of steel is taken as the recycled one [42].

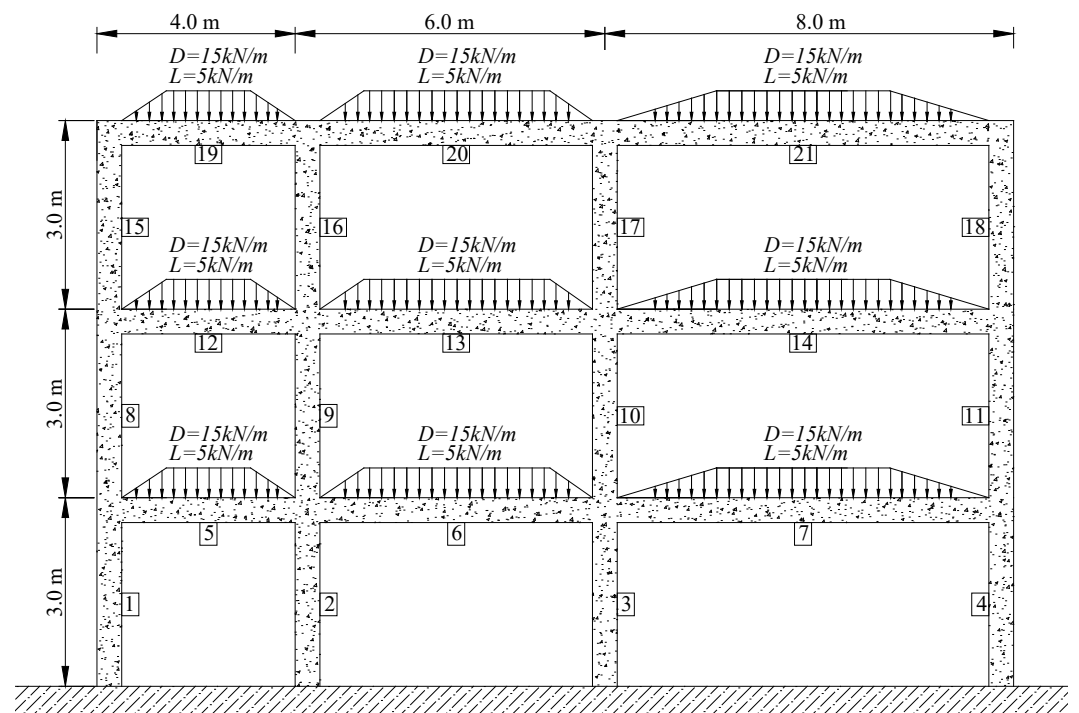


Figure 2. Model of the numerical example.

Table 1. Earthquake records.

Earthquake	Date	Station	Component	PGA(g)
Imperial Valley	1940	117 El Centro	I-ELC180	0.313
Northridge	1994	24514 Sylmar	SYL360	0.843
Loma Prieta	1989	16 LGPC	LGP000	0.563

The optimum results for cost and  $\text{CO}_2$  optimization are shown in Table 3. As seen from cost and  $\text{CO}_2$  values, the exact objective function taken in the optimization process is at the minimum level.

In the optimum design, the breadths of all members were found as the minimum range value. In the search for the optimum results, the optimization process tends to increase the height values, which increase the moment capacity, with a minimum increase in cross-sectional areas that directly affect cost and  $\text{CO}_2$  emission. In cost optimization, several members have greater height values compared to  $\text{CO}_2$  optimization results. This situation is seen for column members.

**Table 2.** Design constants and ranges of design variables.

Definition	Symbol	Unit	Value
Range of web width	$b_w$	mm	250–400
Range of height	$h$	mm	300–600
Clear cover	$c_c$	mm	30
Range of reinforcement	$\phi$	mm	16–30
Range of shear reinforcement	$\phi_v$	mm	8–14
Max. aggregate diameter	$D_{max}$	mm	16
Yield strength of steel	$f_y$	MPa	420
Comp. strength of concrete	$f'_c$	MPa	30
Elasticity modulus of steel	$E_s$	MPa	200,000
Specific gravity of steel	$\gamma_s$	t/m <sup>3</sup>	7.86
Specific gravity of concrete	$\gamma_c$	t/m <sup>3</sup>	2.5
Elastic response parameter	$R$	-	8.5
Cost of concrete per m <sup>3</sup>	$C_c$	\$	50
Cost of steel per ton	$C_s$	\$	750
CO <sub>2</sub> emissions of concrete per m <sup>3</sup>	$C_{c,co2}$	kg	376
CO <sub>2</sub> emissions of steel per ton	$C_{s,co2}$	kg	352

**Table 3.** The optimum results.

Element Number	Cost Optimization		CO <sub>2</sub> Optimization	
	$b_w$ (mm)	$h$ (mm)	$b_w$ (mm)	$h$ (mm)
1	0.25	0.40	0.25	0.30
2	0.25	0.40	0.25	0.35
3	0.25	0.40	0.25	0.35
4	0.25	0.40	0.25	0.30
5	0.25	0.30	0.25	0.30
6	0.25	0.30	0.25	0.30
7	0.25	0.35	0.25	0.35
8	0.25	0.40	0.25	0.30
9	0.25	0.40	0.25	0.30
10	0.25	0.40	0.25	0.30
11	0.25	0.40	0.25	0.30
12	0.25	0.35	0.25	0.35
13	0.25	0.40	0.25	0.40
14	0.25	0.40	0.25	0.40
15	0.25	0.40	0.25	0.30
16	0.25	0.40	0.25	0.30
17	0.25	0.40	0.25	0.30
18	0.25	0.40	0.25	0.30
19	0.25	0.40	0.25	0.40
20	0.25	0.40	0.25	0.40
21	0.25	0.40	0.25	0.40
CO <sub>2</sub> (kg/m <sup>3</sup> )	3597.24		3308.09	
Cost (USD)	1241.62		1260.43	

The optimum results were checked for inter-storey drift values, which ensured that the maximum drift values under three earthquake records in Table 1 are lower than the 2.5% height of the storey, as seen from the maximum drift plots under the critical excitation (LGP000) given in Figure 3. Since the column cross-sectional areas in cost optimization are greater, the maximum drift occurring at the structure is less than the CO<sub>2</sub> optimized structure.

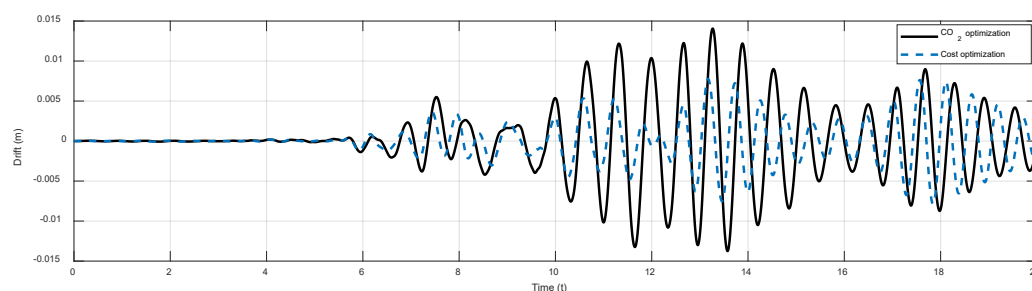


**Figure 3.** The drift plot for the critical excitation.

#### 4. Conclusions

For the eco-friendly design of RC structures, it is aimed to develop an optimization methodology. It provides sustainable development by reducing the CO<sub>2</sub> emission for RC structures. As a complex optimum design, the problem was investigated on RC frame structures. The proposed HS-based modified method was applied in the optimization process. In the numerical examinations, the results of the cost and CO<sub>2</sub> emission minimization were compared with steel, which had the same CO<sub>2</sub> emission value as recycled material.

According to the optimum results presented in Section 3, it is clear to say that the cost and CO<sub>2</sub> minimization, as the optimization objectives, have different optimum designs. For CO<sub>2</sub> emission minimization, it is possible to reduce CO<sub>2</sub> emission by 8% compared to the cost minimization results. This protection of the Earth is only possible with a 1.5% increase in the cost minimization result. Due to this finding, the minimization of CO<sub>2</sub> does not cause a huge expense. In this case, an environmentally friendly optimum design is more feasible than cost optimization, and the usage of recycled material is very suitable for the protection of the Earth with low expense.

According to the results, the proposed algorithm was found to be effective for solving the optimum design problem. In future work, the effect of the cost and CO<sub>2</sub> ratios of concrete and steel can be investigated for site-specific values after data collection from different places in the world according to available materials in the construction region.

**Author Contributions:** G.B. and S.M.N. generated the analysis codes. The text of the paper was formed by G.B., S.M.N., S.K. and Z.W.G. The figures were prepared by G.B. and S.M.N. G.B. and Z.W.G. supervised the research direction. All authors have read and agreed to the published version of the manuscript.

**Funding:** This research received no external funding.

**Institutional Review Board Statement:** Not applicable.

**Informed Consent Statement:** Not applicable.

**Data Availability Statement:** The data about the paper can be requested from corresponding author.

**Conflicts of Interest:** The authors declare no conflict of interest.

#### References

1. Kayabekir, A.E.; Bekdaş, G.; Nigdeli, S.M. *Metaheuristic Approaches for Optimum Design of Reinforced Concrete Structures: Emerging Research and Opportunities*; IGI Global: Hershey, PA, USA, 2020. [\[CrossRef\]](#)
2. Adeli, H.; Sarma, K. *Cost Optimization of Structures—Fuzzy Logic, Genetic Algorithms, and Parallel Computing*; John Wiley and Sons: West Sussex, UK, 2006.
3. Coello, C.C.; Hernandez, F.S.; Farrera, F.A. Optimal Design of Reinforced Concrete Beams Using Genetic Algorithms. *Expert Syst. Appl.* **1997**, *12*, 101–108. [\[CrossRef\]](#)
4. Rafiq, M.Y.; Southcombe, C. Genetic algorithms in optimal design and detailing of reinforced concrete biaxial columns supported by a declarative approach for capacity checking. *Comput. Struct.* **1998**, *69*, 443–457. [\[CrossRef\]](#)
5. Koumoussis, V.K.; Arsenis, S.J. Genetic Algorithms in Optimal Detailed Design of Reinforced Concrete Members. *Comput.-Aided Civ. Inf. Eng.* **1998**, *13*, 43–52. [\[CrossRef\]](#)
6. Rajeev, S.; Krishnamoorthy, C.S. Genetic Algorithm-Based Methodology for Design Optimization of Reinforced Concrete Frames. *Comput.-Aided Civ. Inf. Eng.* **1998**, *13*, 63–74. [\[CrossRef\]](#)

7. Rath, D.P.; Ahlawat, A.S.; Ramaswamy, A. Shape Optimization of RC Flexural Members. *J. Struct. Eng.-ASCE* **1999**, *125*, 1439–1446. [[CrossRef](#)]
8. Camp, C.V.; Pezeshk, S.; Hansson, H. Flexural Design of Reinforced Concrete Frames Using a Genetic Algorithm. *J. Struct. Eng.-ASCE* **2003**, *129*, 105–111. [[CrossRef](#)]
9. Leps, M.; Sejnoha, M. New approach to optimization of reinforced concrete beams. *Comput. Struct.* **2003**, *81*, 1957–1966. [[CrossRef](#)]
10. Lee, C.; Ahn, J. Flexural Design of Reinforced Concrete Frames by Genetic Algorithm. *J. Struct. Eng.-ASCE* **2003**, *129*, 762–774. [[CrossRef](#)]
11. Govindaraj, V.; Ramasamy, J.V. Optimum detailed design of reinforced concrete continuous beams using Genetic Algorithms. *Comput. Struct.* **2005**, *84*, 34–48. [[CrossRef](#)]
12. Sahab, M.G.; Ashour, A.F.; Toropov, V.V. Cost optimization of reinforced concrete flat slab buildings. *Eng. Struct.* **2005**, *27*, 313–322. [[CrossRef](#)]
13. Govindaraj, V.; Ramasamy, J.V. Optimum detailed design of reinforced concrete frames using genetic algorithms. *Eng. Optimiz.* **2007**, *39*, 471–494. [[CrossRef](#)]
14. Park, H.S.; Kwon, B.; Shin, Y.; Kim, Y.; Hong, T.; Choi, S.W. Cost and CO<sub>2</sub> emission optimization of steel reinforced concrete columns in high-rise buildings. *Energies* **2013**, *6*, 5609–5624. [[CrossRef](#)]
15. Lee, M.S.; Hong, K.; Choi, S.W. Genetic Algorithm Based Optimal Structural Design Method for Cost and CO<sub>2</sub> Emissions of Reinforced Concrete Frames. *J. Comput. Struct. Eng. Inst. Korea* **2016**, *29*, 429–436. [[CrossRef](#)]
16. Mergos, P.E. Seismic design of reinforced concrete frames for minimum embodied CO<sub>2</sub> emissions. *Energy Build.* **2018**, *162*, 177–186. [[CrossRef](#)]
17. Akin, A.; Saka, M.P. Harmony search algorithm based optimum detailed design of reinforced concrete plane frames subject to ACI 318-05 provisions. *Comput. Struct.* **2015**, *147*, 79–95. [[CrossRef](#)]
18. American Concrete Institute Committee. *ACI 318-14, Building Code Requirements for Structural Concrete and Commentary*; American Concrete Institute: Farmington Hills, MI, USA, 2014.
19. Nigdeli, S.M.; Bekdas, G.; Kim, S.; Geem, Z.W. A novel harmony search based optimization of reinforced concrete biaxially loaded columns. *Struct. Eng. Mech. Int. J.* **2015**, *54*, 1097–1109. [[CrossRef](#)]
20. Bekdas, G. Harmony search algorithm approach for optimum design of post-tensioned axially symmetric cylindrical reinforced concrete walls. *J. Optim. Theory Appl.* **2015**, *164*, 342–358. [[CrossRef](#)]
21. Garcia-Segura, T.; Yepes, V.; Alcalá, J.; Pérez-López, E. Hybrid harmony search for sustainable design of post-tensioned concrete box-girder pedestrian bridges. *Eng. Struct.* **2015**, *92*, 112–122. [[CrossRef](#)]
22. Bekdas, G.; Nigdeli, S.M. Modified harmony search for optimization of reinforced concrete frames. In Proceedings of the 3rd International Conference on the Harmony Search Algorithm, Bilbao, Spain, 22–24 February 2017; Springer: Singapore, 2017; pp. 213–221.
23. Medeiros, G.F.; Kripka, M. Modified harmony search and its application to cost minimization of RC columns. *Adv. Comput. Des.* **2017**, *2*, 1–13. [[CrossRef](#)]
24. Shaqfa, M.; Orbán, Z. Modified parameter-setting-free harmony search (PSFHS) algorithm for optimizing the design of reinforced concrete beams. *Struct. Multidiscip. Optim.* **2019**, *60*, 999–1019. [[CrossRef](#)]
25. Kayabekir, A.E.; Arama, Z.A.; Bekdas, G.; Nigdeli, S.M.; Geem, Z.W. Eco-friendly design of reinforced concrete retaining walls: Multi-objective optimization with harmony search applications. *Sustainability* **2020**, *12*, 6087. [[CrossRef](#)]
26. Yücel, M.; Kayabekir, A.E.; Bekdas, G.; Nigdeli, S.M.; Kim, S.; Geem, Z.W. Adaptive-Hybrid Harmony Search Algorithm for Multi-Constrained Optimum Eco-Design of Reinforced Concrete Retaining Walls. *Sustainability* **2021**, *13*, 1639. [[CrossRef](#)]
27. Bekdas, G.; Arama, Z.A.; Kayabekir, A.E.; Geem, Z.W. Optimal design of cantilever soldier pile retaining walls embedded in frictional soils with harmony search algorithm. *Appl. Sci.* **2020**, *10*, 3232. [[CrossRef](#)]
28. Arama, Z.A.; Kayabekir, A.E.; Bekdas, G.; Geem, Z.W. CO<sub>2</sub> and cost optimization of reinforced concrete cantilever soldier piles: A parametric study with harmony search algorithm. *Sustainability* **2020**, *12*, 5906. [[CrossRef](#)]
29. Kayabekir, A.E.; Nigdeli, S.M.; Bekdas, G. Adaptive Harmony Search for Cost Optimization of Reinforced Concrete Columns. In Proceedings of the International Conference on Intelligent Computing & Optimization, Hua Lin, Thailand, 30–31 December 2021; Springer: Cham, Switzerland, 2021; pp. 35–44.
30. Nigdeli, S.M.; Bekdas, G.; Yang, X.S. Metaheuristic optimization of reinforced concrete footings. *KSCE J. Civ. Eng.* **2018**, *22*, 4555–4563. [[CrossRef](#)]
31. Esfandiari, M.J.; Urgessa, G.S.; Sheikholarefin, S.; Manshadi, S.D. Optimization of reinforced concrete frames subjected to historical time-history loadings using DMPHO algorithm. *Struct. Multidiscip. Optim.* **2018**, *58*, 2119–2134. [[CrossRef](#)]
32. Afshari, H.; Hare, W.; Tesfamariam, S. Constrained multi-objective optimization algorithms: Review and comparison with application in reinforced concrete structures. *Appl. Soft Comput.* **2019**, *83*, 105631. [[CrossRef](#)]
33. Mergos, P.E.; Mantoglou, F. Optimum design of reinforced concrete retaining walls with the flower pollination algorithm. *Struct. Multidiscip. Optim.* **2020**, *61*, 575–585. [[CrossRef](#)]
34. Esra, U.R.A.Y.; Çarbaş, S. Dynamic Loads and Different Soil Characteristics Examination on Optimum Design of Cantilever Retaining Walls Utilizing Harmony Search Algorithm. *Int. J. Eng. Appl. Sci.* **2021**, *13*, 140–154.
35. Sánchez-Olivares, G.; Tomás, A. Optimization of Reinforced Concrete Sections under Compression and Biaxial Bending by Using a Parallel Firefly Algorithm. *Appl. Sci.* **2021**, *11*, 2076. [[CrossRef](#)]

36. Camp, C.V.; Assadollahi, A. CO<sub>2</sub> and cost optimization of reinforced concrete footings using a hybrid big bang-big crunch algorithm. *Struct. Multidiscip. Optim.* **2013**, *48*, 411–426. [[CrossRef](#)]
37. Paya-Zaforteza, I.; Yepes, V.; Hospitaler, A.; Gonzalez-Vidosa, F. CO<sub>2</sub>-optimization of reinforced concrete frames by simulated annealing. *Eng. Struct.* **2009**, *31*, 1501–1508. [[CrossRef](#)]
38. Camp, C.V.; Huq, F. CO<sub>2</sub> and cost optimization of reinforced concrete frames using a big bang-big crunch algorithm. *Eng. Struct.* **2013**, *48*, 363–372. [[CrossRef](#)]
39. Geem, Z.W.; Kim, J.H.; Loganathan, G.V. Harmony search optimization: Application to pipe network design. *Int. J. Model. Simul.* **2002**, *22*, 125–133. [[CrossRef](#)]
40. Mathworks, *MATLAB R2010a*; The MathWorks Inc.: Natick, MA, USA, 2010.
41. PEER. Pacific Earthquake Engineering Resource Center: NGA Database. University of California, Berkeley. 2005. Available online: <http://peer.berkeley.edu/nga> (accessed on 10 November 2011).
42. Yeo, D.H.; Potra, F.A. Sustainable design of reinforced concrete structures through CO<sub>2</sub> emission optimization. *J. Struct. Eng.* **2015**, *141*, 3. [[CrossRef](#)]